Nat. Hazards Earth Syst. Sci., 21, 2257–2276, 2021
https://doi.org/10.5194/nhess-21-2257-2021

Natural Hazards and Earth System Sciences
Open Access
EGU

Deep uncertainties in shoreline change projections: an extra-probabilistic approach applied to sandy beaches

Rémi Thiéblemont[1], Gonéri Le Cozannet[1], Jérémy Rohmer[1], Alexandra Toimil[2], Moisés Álvarez-Cuesta[2], and Iñigo J. Losada[2]

[1]Bureau de Recherches Géologiques et Minières "BRGM", French Geological Survey, 3 Avenue, Claude Guillemin, CEDEX, 45060 Orléans, France
[2]IHCantabria-Instituto de Hidráulica Ambiental de la Universidad de Cantabria, Parque Científico y Tecnológico de Cantabria, Calle Isabel Torres 15, 39011 Santander, Cantabria, Spain

Correspondence: Rémi Thiéblemont (r.thieblemont@brgm.fr)

Received: 15 December 2020 – Discussion started: 13 January 2021
Revised: 7 May 2021 – Accepted: 21 May 2021 – Published: 30 July 2021

Abstract. Global mean sea level rise and its acceleration are projected to aggravate coastal erosion over the 21st century, which constitutes a major challenge for coastal adaptation. Projections of shoreline retreat are highly uncertain, however, namely due to deeply uncertain mean sea level projections and the absence of consensus on a coastal impact model. An improved understanding and a better quantification of these sources of deep uncertainty are hence required to improve coastal risk management and inform adaptation decisions. In this work we present and apply a new extra-probabilistic framework to develop shoreline change projections of sandy coasts that allows consideration of intrinsic (or aleatory) and knowledge-based (or epistemic) uncertainties exhaustively and transparently. This framework builds upon an empirical shoreline change model to which we ascribe possibility functions to represent deeply uncertain variables. The model is applied to two local sites in Aquitaine (France) and Castellón (Spain). First, we validate the framework against historical shoreline observations and then develop shoreline change projections that account for possible (although unlikely) low-end and high-end mean sea level scenarios. Our high-end projections show for instance that shoreline retreats of up to 200 m in Aquitaine and 130 m in Castellón are plausible by 2100, while low-end projections revealed that 58 and 37 m modest shoreline retreats, respectively, are also plausible. Such extended intervals of possible future shoreline changes reflect an ambiguity in the probabilistic description of shoreline change projections, which could be substantially reduced by better constraining sea level rise (SLR) projections and improving coastal impact models. We found for instance that if mean sea level by 2100 does not exceed 1 m, the ambiguity can be reduced by more than 50 %. This could be achieved through an ambitious climate mitigation policy and improved knowledge on ice sheets.

1 Introduction

Global mean sea level rose over the period 2006–2015 at a rate more than 2 times larger than over the whole 20th century and is projected to continue rising for the centuries to come (Oppenheimer et al., 2019). This inevitable sea level rise (SLR) will exacerbate risks in coastal areas, notably erosion and flooding. Recent analysis of satellite-derived shoreline changes has revealed that a quarter of the world's sandy beaches are eroding (Luijendijk et al., 2018) and that the overall surface of eroded land recorded over the period 1984–2015 (about 28 000 km^2) is 2 times larger than the surface of gained land (Mentaschi et al., 2018). This situation is projected to worsen with climate change (Ranasinghe, 2016; Vousdoukas et al., 2020). Yet, future coastal retreat projections are highly uncertain, reflecting the deep uncertainties of future sea level rise projections and of coastal impact models (Le Cozannet et al., 2019a; Athanasiou et al., 2020; Ranasinghe, 2020; Cooper et al., 2020; Vershuur et al., 2020). An improved understanding and a better quantification of these sources of uncertainty are required to improve coastal risk

management and inform adaptation decisions (Stephens et al., 2017).

Since the release of the Fifth Assessment Report (AR5) of the Intergovernmental Panel on Climate Change (IPCC) (Church et al., 2013), SLR projections by 2100 have been reassessed upwards, and the range of uncertainty has enlarged for scenarios of high greenhouse gas emissions (Oppenheimer et al., 2019). This update of IPCC SLR projections is due to the consideration of marine ice sheet instabilities (Joughin et al., 2014; Rignot et al., 2014). Hence, the IPCC Special Report on The Ocean and Cryosphere in a changing Climate (SROCC) revised the median SLR by 2100 to 0.84 m for the RCP8.5 scenario (instead of 0.74 m of the AR5), and the upper limit of the likely range jumped to 1.1 m (instead of 0.98 m).

In addition, the SLR projections delivered by the IPCC do not cover the whole range of uncertainties. In fact, future ice sheet contributions remain deeply uncertain, as a collapse of the west Antarctic ice sheet during the 20th century cannot be excluded yet (DeConto and Pollard, 2016; Edwards et al., 2019). Hence, the possibility of future SLR projections being above or below the IPCC likely range remains. Evidence for the possibility of large ice sheet contribution to sea level rise include, e.g., physical modelling of melting processes (DeConto and Pollard, 2016) and structured expert judgement (Bamber et al., 2019). For example, Bamber et al. (2019) found that SLR could exceed 2 m by 2100 for a high-emission scenario (lying within the 90 % uncertainty bounds), reflecting at least the absence of consensus within the community of glaciologists. Importantly, the gravitational effects of large ice sheet mass losses mean that sea level rise would exceed the global mean along most inhabited shorelines. For example, Thiéblemont et al. (2019) showed that given the current ocean and cryosphere physically based projections, the SLR could possibly – although unlikely – be as high as 1.9 m off the coasts of western Europe by 2100 under the RCP8.5 scenario. The deep uncertainty associated with future regional sea level change reflects the incomplete understanding of the underlying physical processes but also the uncertain magnitude of global warming in the future.

Coastal impact models used to project the shoreline change response to sea level rise are another major source of uncertainty (Ranasinghe, 2016, 2020; Toimil et al., 2020). Shoreline changes are controlled by multiple hydro-sedimentary processes that interact with each other and operate at multiple timescales (ranging from 1 d to several decades) and spatial scales (Stive et al., 2002). Processes driving shoreline change are also extremely variable from one beach segment to another, making very challenging the development of a standardised process-based modelling framework. Although numerical models have demonstrated significant skilful predictions of shoreline changes (Montaño et al., 2020), their use is generally restricted to local applications where high-resolution and high-accuracy data (e.g. topo-bathymetry, nearshore hydrodynamics, sediment characteristics) are available (Robinet et al., 2018; Enríquez et al., 2019). At a large scale (generally > 500 km), assessments of shoreline change projections (Hinkel et al., 2019; Thiéblemont et al., 2019; Vousdoukas et al., 2020; Athanasiou et al., 2020) rely widely on the Bruun rule, a two-dimensional cross-shore model that predicts landward retreat of the shoreline in response to SLR assuming a conserved equilibrium beach profile (Bruun, 1962). Nonetheless, the usefulness of the Bruun rule as a predictive tool is highly debated, notably with regard to its lack of validation against observations, robustness, and general applicability, as beach segments generally do not meet the assumptions for the Bruun rule application (Stive, 2004; Cooper and Pilkey, 2004; Ranasinghe and Stive, 2009; Ranasinghe, 2016; Cooper et al., 2020). For example, several studies found that the Bruun rule tends to provide substantially higher shoreline retreat projections than physics-based probabilistic shoreline change models (Ranasinghe et al., 2012; Toimil et al., 2017; Le Cozannet et al., 2019a; Enríquez et al., 2019).

This deep uncertainty context inherent to shoreline change projections is a major challenge for coastal management and adaptation decisions. Hinkel et al. (2019) showed that different kinds of information on sea level projections are required depending namely on the time horizon of coastal decision adaptation and on the degree of uncertainty tolerance of users. For medium to high uncertainty tolerance, probabilistic projections are particularly well suited to identify the adaptation alternative that has the best-expected outcome (Nicholls et al., 2014; Budescu et al., 2014). In contrast, when uncertainty tolerance is low, robust decision-making is preferable, which implies testing adaptation options against any plausible scenarios, hence considering high-end (Hinkel et al., 2015, 2019; Kopp et al., 2017; Stammer et al., 2019) and low-end (Le Cozannet et al., 2019b) projections (or scenarios), which explore plausible – although unlikely – upper- and lower-tail sea level scenarios beyond the likely range. Although the literature above has focused on sea level rise information needs, the same type of information is needed for its coastal impacts (Rohmer et al., 2019), raising the need for a framework allowing the propagation and analysis of deep uncertainties from sea level rise to its impacts.

To develop shoreline change projections that meet the needs of users with various risk tolerances, different future scenarios need to be developed and combined with a large variety of sources of uncertainty. Two types of uncertainty need to be considered (Beven et al., 2018; Toimil et al., 2020): intrinsic uncertainty (also called aleatory), which is inherent to the considered process (e.g. internal variability) and knowledge-based uncertainty (also called epistemic), which stems from information incompleteness or lack of knowledge (incl. deep uncertainties). To date, both types of uncertainties have been addressed mainly using the tools provided by the probability theory and occasionally used in combination with expert knowledge (especially for sea level projections; Oppenheimer et al., 2019; Bamber et al., 2019). Yet, several

studies have pointed out that the use of probabilities merges the different uncertainty types in a single format and can in turn induce an appearance of overconfidence in uncertainty quantification (Le Cozannet et al., 2017; van der Pol and Hinkel, 2019; Bakker et al., 2017; Rohmer et al., 2019). Such a misleading effect can have a serious impact on coastal risk management and planning. To overcome this disadvantage of the classical probabilistic setting, alternative mathematical representation methods have been developed (see a comprehensive overview by Dubois and Guyonnet, 2011). These are termed extra-probabilistic because they avoid the selection of a single probability law by bounding all the possible probability models consistent with the available data. The added value of these approaches has been discussed for global SLR projections (Le Cozannet et al., 2017) or to assess local flood impact (Rohmer et al., 2019) but has never been used in the context of coastal erosion to our knowledge.

In this paper, we build on the extra-probabilistic framework of uncertainty to develop a new and versatile modelling framework to project future shoreline changes of sandy beaches. This framework enables coastal risk managers to account exhaustively and transparently for uncertainty of different kinds (aleatory and epistemic) and more specifically for deep uncertainty by providing the necessary tools to quantify it (via the definition of high-end and low-end scenarios) to support various decision contexts. Section 2 describes the shoreline change extra-probabilistic framework development. Section 3 describes the physical characteristics of the two study sites and the associated data. In Sect. 4, we validate the shoreline change modelling framework against historical records and then use them for future projections. Our results are further discussed in Sect. 5.

2 Extra-probabilistic framework for shoreline change projections

2.1 Extra-probabilistic framework: general principle

Uncertainty representation consists of modelling the available knowledge, i.e. selecting the most appropriate mathematical tools and procedures for representing the available data/information while "accounting for all data and pieces of information, but without introducing unwarranted assumptions" (Beer et al., 2013). When a large number of observations are available, a probability distribution can be inferred from data/observations. In our case, this applies for instance to the mean sea level in the Bay of Biscay over the recent historical period, for which several observational records from tide gauges exist. In situations where the data and information are very scarce, imprecise, vague, even incomplete (i.e. an environment of imperfect knowledge; Beer et al., 2013), selecting an appropriate probability law can be ambiguous. The later issue is referred to as deep uncertainties in the literature and can be addressed quantitatively by extra-probabilistic methods (Dubois and Guyonnet, 2011).

Extra-probabilistic theories of uncertainty recognise that several probabilistic laws may exist given the piece of information available. Instead of providing a single uncertainty (probabilistic) model, they deliver sets of plausible probabilistic models. In the present study, we use the possibility theory to represent uncertainties of deeply uncertain variables (Dubois and Prade, 1988). The basic ingredient is the interval used for representing experts' knowledge. In most cases, however, experts may provide more information by expressing preferences within this interval. Such "nuanced" information can be conveyed using the possibility distributions, denoted π (Dubois and Prade, 1988), which describe the more or less plausible values of some uncertain quantity. The intervals defined as $\pi_\alpha = \{e, \pi(e) \geq \alpha\}$ are called α-cuts. They contain all the values that have a degree of possibility of at least α (lying between 0 and 1). The example of an α-cut on a trapezoid possibility distribution is shown in Fig. 1a. The interval for $\alpha = 0$ and $\alpha = 1$ is called the support and the core, respectively. The α-cuts formally correspond to the confidence interval $1-\alpha$ as traditionally defined in the probability theory, i.e $\text{Prob}(e \in \pi_\alpha) \geq 1-\alpha$. Thus, a possibility distribution can be interpreted as a set of nested intervals, each of them being assigned with a level of confidence $1-\alpha$. A possibility distribution then encodes a family of probability laws (Dubois and Prade, 1992), i.e. a probability box limited by an upper probability bound called the possibility measure $\prod(e \in E) = \sup_{e \in E} \pi(e)$ (upper cumulative probability bound in Fig. 1b) and a lower probability bound called the necessity measure $N(e \in E) = \inf_{e \notin E}(1-\pi(e))$, where E represents a specific interval ($E =]1.0, +\infty[$ for instance). This link between probabilistic and possibilistic theories was exploited by Le Cozannet et al. (2017) to derive a possibility distribution to represent uncertainties on GSLR (global sea level rise) by 2100 conditional on the RCP8.5 scenario.

2.2 Setting up shoreline change projections within the extra-probabilistic framework

In principle, the extra-probabilistic framework can be used with any shoreline change model. In this study, we adopt the perspective of coastal adaptation practitioners that generally rely on empirical models that extrapolate observed shoreline changes to better anticipate their future evolution (Peter et al., 2003; Le Cozannet et al., 2019a; Vousdoukas et al., 2020; Cowell et al., 2003). In the absence of estuaries or other major sediment sources or sinks, our empirical model expresses shoreline change ΔS following Eq. (1):

$$\Delta S = S_t - S_{t0} = \frac{\Delta \text{RSLC}}{\tan \beta} + \text{Lvar} + n \cdot \text{Tx}, \quad (1)$$

where $S_t - S_{t0}$ expresses the change in shoreline position in the cross-shore direction from reference time t_0 to time t;

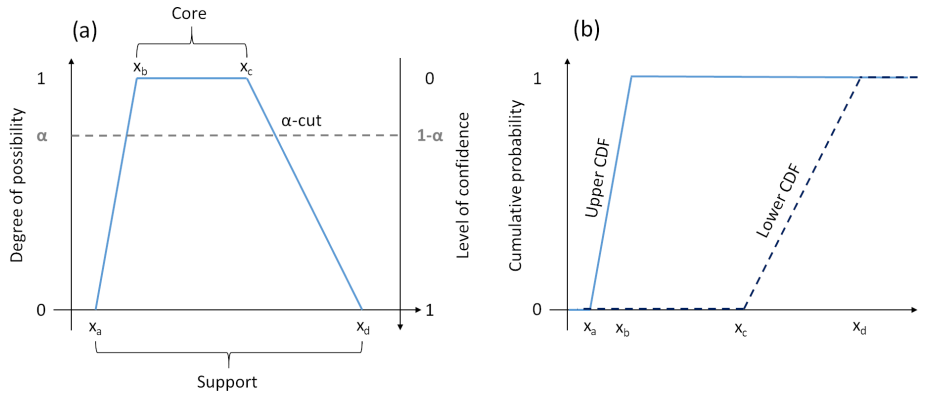

Figure 1. Example of **(a)** trapezoidal possibility distribution and **(b)** its translation into a probability box.

$(\Delta\mathrm{RSLC})/(\tan\beta)$ quantifies the contribution of sea level rise to shoreline changes, which takes the form of the Bruun rule (Bruun, 1962); Tx is the linear trend of shoreline changes over multi-decadal timescales and n the number of years relative to the baseline; and Lvar characterises the interannual to decadal variability of shoreline change: typically, Lvar would quantify how the shoreline can depart from a mean position due to, e.g., seasonal cycles or the chronological sequence of storms and calm periods. These terms, which are described further below, include intrinsic and knowledge uncertainties that need to be adequately represented as input and then propagated. The flowchart in Fig. 2 displays the three steps to develop shoreline change projections within the extra-probabilistic framework.

As a first step (Fig. 2a and b), uncertainty distribution of inputs is constructed. For instance, in Eq. (1), $n \cdot \mathrm{Tx}$ and Lvar are both derived from past shoreline change observations. Note that the Tx and Lvar terms do not describe a single physical process but rather a combination of processes that operate at different timescales including wave climates, sediment budgets, effects of longshore gradients in sediment transport or anthropogenic actions. These processes are recognised as complex and difficult to model with reduced-complexity models (Montaño et al., 2020; Vitousek et al., 2017). By using the empirical model, our objective is to reproduce the observed trends and modes of variability without trying to model the physical processes explicitly, while keeping a low computation time (see Helgeson et al., 2020, for a broader discussion of this approach). The term $n \cdot \mathrm{Tx}$ is the product of the number of years n since the reference year and the multi-decadal linear trend Tx derived from observations after subtracting the effect of sea level rise. In the case where multiple observations are available per year (typically when analysing shoreline changes retrieved from satellite imagery), the linear model used to derive Tx is applied to annual means and weighted by the number of samples per year to account for the irregularity of the temporal sampling (see e.g. Fig. 4b). The residuals of the linear regression to compute Tx are then used to derive Lvar. We sample residuals that are distant by a gap of N years (with $1 < N < 10$ as we focus on interannual to decadal timescales) and compute their standard deviation. This procedure is repeated for all possible combinations of residuals separated by N years. Finally, Lvar is determined as the maximum standard deviation value obtained among all samples. Note that Lvar is found to maximise for $N \geq 5$ years. Since Tx and Lvar are derived assuming that errors of the linear regression are normally distributed, they are both prescribed as probability distributions.

In contrast, terms accounting for future sea level (ΔRSLR) and its impact on shoreline change ($1/\tan\beta$) are both sources of deep uncertainty and are therefore too imprecise given the current knowledge to be constrained by probability distributions. For instance, to reflect the full range of current uncertainty, ΔRSLR should consider projections that are either below or beyond the likely range provided by the IPCC, but for which probability is not well established. Regarding the coastal impact model, under the Bruun rule (Bruun, 1962), $\tan\beta$ corresponds to the slope of the active profile from the depth of closure to the top of the upper shoreface. The Bruun rule's underlying assumptions include considering that sediment transport only occurs perpendicularly to the shoreline, thus neglecting any tri-dimensional variability, and assuming that the coastal profile is an equilibrium profile that has uniform sediment size. An alternative to the Bruun rule was proposed through the probabilistic coastline recession (PCR) model (Ranasinghe et al., 2012). The PCR model quantifies sediment losses at the dune toe during storms, as well as the nourishment of the dune by aeolian sediment transport processes between storms. Given a certain amount of sea level rise, the response of the PCR model is less erosive than the Bruun rule by 1 order of magnitude. While the use of the PCR model is rather expensive computationally, Le Cozannet et al. (2019a) demonstrated that, in a first approximation, the equilibrium response of the PCR model can be emulated in Eq. (1) by replacing the nearshore slopes (or Bruun slopes) by the foreshore slopes. Bruun and PCR models are however both difficult to validate because of the scarcity of coastal data and the complexity of the hydrosedimentary processes

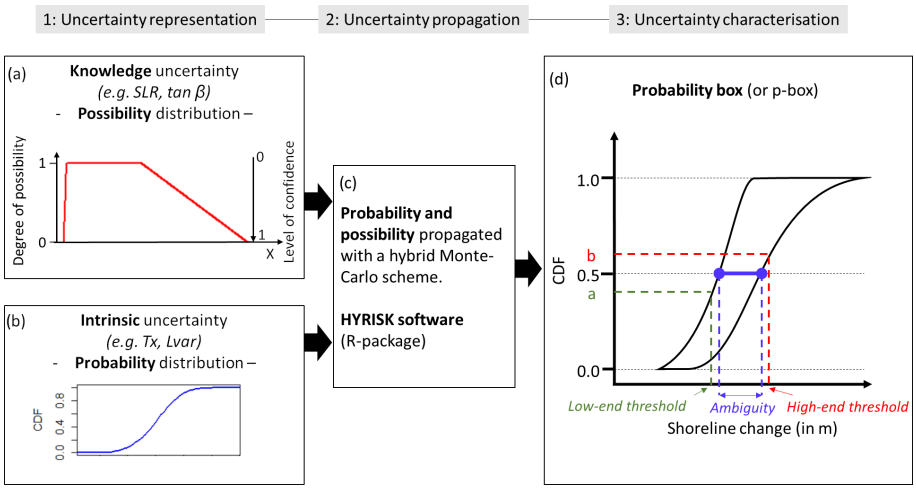

Figure 2. Schematisation of the framework used herein to perform future shoreline change projections within the extra-probabilistic theory.

involved. This constitutes one of the sources of deep uncertainty. Hence, to reflect the absence of consensus on coastal erosion induced by sea level rise, neither the surrogate PCR model nor the Bruun rule should be discarded in our uncertainty propagation. To account for the limited knowledge of future sea level and its impact on shoreline change, we construct ΔRSLR and $1/\tan\beta$ terms as trapezoidal possibility distributions (see also Sect. 4a and b).

As a second step (Fig. 2b), to propagate the heterogeneous uncertainty nature of the terms in Eq. (1), we used the HYRISK R package (Rohmer et al., 2018). HYRISK software is designed to jointly propagate probability and possibility by implementing the hybrid Monte Carlo scheme, named the independent random sampling (IRS) algorithm developed by Baudrit et al. (2005). The IRS algorithm combines random sampling of the inverse of the cumulative probability distribution functions for random parameters and the α-cuts (intervals associated with a level of confidence of $1-\alpha$) from the possibility distributions. More details on the IRS algorithm are provided in Appendix A. The result of the propagation procedure takes the form of random intervals that can be summarised by pairs of upper and lower cumulative probability distributions (CDFs), which allows construction of probability boxes (or p boxes, final step) based on the formal setting introduced by Baudrit et al. (2007).

Figure 2d shows a typical example of shoreline change uncertainty propagation presented in the form of a p box. The p box is bounded to the left and right by the upper and lower CDFs, respectively. The area enclosed within these two bounds includes all possible distributions of shoreline changes and characterises the full range of aleatoric and epistemic uncertainties. Epistemic uncertainty is represented by the breadth between the upper and lower CDFs, whereas aleatory uncertainty is represented by the overall tilt of the p box. The gap between the upper and lower CDFs can be considered "what is unknown" and represents the imperfect state of knowledge (Rohmer et al., 2019). To quantify this deep uncertainty, we use an indicator termed "ambiguity" and defined as the width (in metres) between medians of the upper and lower CDFs. In addition, we define the low-end threshold (i.e. minimum adaptation needs, shown in green) as the shoreline change value for which there is a chance smaller than a to be reached under the less impacting (i.e. upper) CDF. In other words, the low-end value corresponds to a threshold, which is very likely to be exceeded. Finally, we define the high-end threshold (i.e. highly risk-adverse applications, shown in red) as the value below which there is still more than b chance for the projections to hold under the most impacting (i.e. lower) CDF. In this case, the high-end threshold corresponds to a value which can be possible but unlikely exceeded. As an example, we define a and b as 0.4 and 0.6, respectively, although these thresholds are meant to be tailored to user needs depending on their risk aversion.

3 Case studies and data

In this work, the extra-probabilistic approach to perform shoreline change projections is applied in two coastal sites where the coastline is largely dominated by sandy beaches (Fig. 3) but (i) for which we have different sources of shoreline change observations and sampling and (ii) that have highly distinct geomorphologic and hydrodynamical characteristics. Thereinafter, positive and negative values represent erosion and accretion, respectively, with respect to the baseline (i.e. 2015 for site 1 in Aquitaine and 2020 for site 2 in Castellón).

3.1 Case studies and shoreline change observational records

The first site studied (site 1) is located in the municipality of Naujac-sur-Mer, which belongs to the Aquitaine coast

Figure 3. Location of the two case studies on the Aquitaine (site 1, **b**) and Castellón (site 2, **c**) coasts. Base maps are from Google Earth.

(Fig. 3). The Aquitaine is a 230 km long sandy coast located in south-western France constituted by high-energy meso-macrotidal open beaches, which are backed by coastal dunes with a typical height ranging between 15 and 20 m and a width larger than 100 m. The characteristic sediment of this coast is well-sorted sand, of medium to fine grain size between 250 and 300 µm. Observational records of spatial and temporal shoreline change along the Aquitanian coast have been retrieved by Castelle et al. (2018). Their shoreline change dataset was generated based on 15 georeferenced orthomosaic photos to examine long-term shoreline change from 1950 to 2014 along 270 km distributed over 2861 transects. They found a spatially averaged erosion trend of 1.1 m yr^{-1} derived throughout the Aquitanian coast with maximum retreat (accretion) rates of 11 (-6) m yr^{-1}. Here, the site studied (Fig. 3b) has been chosen to avoid influence of estuarine processes. Its observational records of shoreline change are shown in Fig. 4a. We found for this individual profile an erosion trend of 0.82 m yr^{-1}, which is close to the time and Aquitanian spatially averaged erosion trend of 1.1 m yr^{-1}.

The second site studied (site 2) is in the Chilches municipality, located on the Mediterranean coast of Spain in the province of Castellón (Fig. 3c). The current coastal morphology in this area is highly conditioned by a succession of anthropic actions that started at the beginning of the 20th century. The construction of the ports of Castellón, Burriana and Sagunto completely blocked the northern contribution of sediments to downdrift of the structures. As a result, the coast shifted from the state of dynamic equilibrium with intense longshore transport and continuous sediment intake to imbalance, with the same longshore transport intensity but without any sediment contribution updrift. This resulted in the chronic recession of the beaches sheltered by the structures and the accretion of the beaches located downdrift. In addition, the real estate boom that occurred in the second half of the 20th century exacerbated such imbalance, giving rise to constructions on beaches that were already in decline. Subsequently, to try to solve this problem, more actions were taken, including the construction of seawalls and jetties and replenishments. In their natural state, these are beaches of fine to medium sand with D_{50} between 0.2–0.35 mm. Shoreline evolution in the Castellón–Sagunto stretch was retrieved using the CoastSat toolkit (Vos et al., 2019b) based on monthly or bimonthly observations from Landsat 5, Landsat 8 and Sentinel 2. CoastSat has been shown to have a particularly high accuracy in microtidal environments (Vos et al., 2019a). For the Castellón–Sagunto stretch, the dataset retrieved by CoastSat has been validated against discrete profile surveys at some specific sites. The shoreline evolution over the period 1989–2019 for the profile studied in Chilches is shown in Fig. 4b. Over the 31-year period, 859 shoreline positions (orange time series) were retrieved for this profile, with an average of 25 (70) observational records per year before (after) 2017. The profile shows an average coastline retreat of 0.6 m yr^{-1} over the period 1989–2019.

In Aquitaine (site 1), topographic and bathymetric surveys recorded nearshore slopes in the range 1.2 %–1.5 % that can

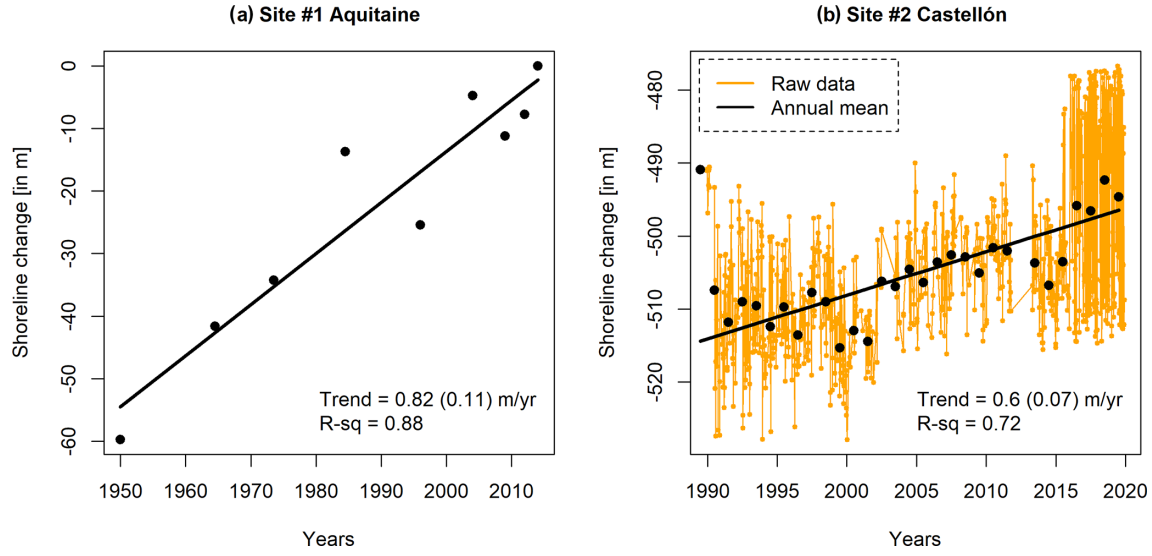

Figure 4. Observed shoreline change evolution in **(a)** site no. 1 in Aquitaine and **(b)** site no. 2 in Castellón. In Castellón, 859 available observations (orange line) and annual averages (black dots) are shown. The black line shows the linear trends calculated from the annual averages, and their standard error is written in brackets. Note that, by convention, positive trend values indicate shoreline retreat.

occasionally be as mild as 1 % (Bernon et al., 2016) and slopes of the upper shoreface that can be as steep as ∼ 10 % (Bulteau et al., 2014). In Castellón, beach slopes have been determined by combining two datasets: a topography dataset from the Spanish Geographic Institute (Instituto Geográfico Nacional, IGN) and a bathymetry dataset from the Spanish Ministry for the Ecological Transition and Demographic Challenge (Ministerio para la Transición Ecológica y el Reto Demográfico, MITERD). Specifically in site 2, a nearshore slope of 3.1 % was retrieved.

3.2 Historical sea level and projections

For both sites, the absolute sea level time evolution in the past is constructed from tide gauge records which are corrected from vertical land motion based on Global Navigation Satellite System (GNSS) station records or global isostatic adjustment models (if GNSS stations are not found nearby). For the Aquitanian coastline, Bay of Biscay past sea level is derived as the average of 15 stations available in the Permanent Service for Mean Sea Level (PSMSL) (see Le Cozannet et al., 2019a, for details). For the Castellón area, and in general along the east coast of Spain, tide gauge records provided in PSMSL are short and do not span the entire time period considered here (i.e. 1989–2019). Therefore, we relied on the Marseille tide gauge (GNSS-corrected) records calculated over the period 1989–2019.

To obtain RSLC regional projections and their related uncertainty, we combine the future regional contributions of stereodynamic effects, melting of mountain glaciers and ice sheets, land water, and glacial isostatic adjustment (Slangen et al., 2012, 2014; Gregory et al., 2019) following the procedure described in Chapter 13 of the IPCC AR5 (Church et al., 2013). Regional projections of the stereodynamic component, which corresponds to changes in ocean density and circulation corrected from the inverse barometer effect, are derived from the outputs of the global climate model simulations performed within the 5th phase of the Coupled Model Intercomparison Project (CMIP5). Note however that our stereodynamic projections slightly deviate from the IPCC AR5 and SROCC procedure.

- Among the 21 CMIP5 models available, MIROC-ESM and MIROC-ESM-CHEM models are discarded as they project an anomalously large stereodynamic component in the Atlantic Ocean and North Sea areas, such that if both models are retained, the distribution of the multi-model ensemble is no longer Gaussian (Thiéblemont et al., 2019). Le Cozannet et al. (2019b) have also shown that by 2100 the global-mean thermosteric sea level rise of these two models (0.5 m for the RCP8.5 scenario) exceeds the median global-mean thermosteric sea level rise of all other models (0.3 m) beyond 5 sigma.

- In the semi-enclosed basins (e.g. Mediterranean Sea), the rather coarse resolution of atmosphere–ocean general circulation models (AOGCMs) prevents an accurate representation of small-scale processes (e.g. water exchange at Gibraltar), which in turn affects regional sea level estimates (Marcos and Tsimplis, 2008; Slangen et al., 2017). The Mediterranean stereodynamic sea level projections are therefore estimated by relying on those of the Atlantic area near Gibraltar, which is the Mediterranean Sea entry point.

For other mass contributions to sea level (i.e. glaciers, ice sheets, land water), regional changes are obtained by downscaling global estimates and their uncertainty using barystatic-GRD (gravity rotation deformation) fingerprints (Gregory et al., 2019). Finally, the regional RSLC likely range is computed as the square root of the sum of the squares of each regionalised component's likely range (except for contributions that correlate with global-mean air temperature – see Church et al., 2013, for details). Stereodynamic sea level projections and barystatic-GRD fingerprints are available from the Integrated Climate Data Center of the University of Hamburg (http://icdc.cen.uni-hamburg.de/, last access: 2 May 2021) (Carson et al., 2016).

To account for deep uncertainty in SLR, we not only restrict to likely range estimates but also consider low- and high-end estimates for the design of our RSLC projections. There is low confidence that sea level rise can reach such values, yet they cannot be discarded. There is no unique approach to design low- and high-end scenarios, as reflected by the recent literature that abounds in sea level projections that explicitly included high-end scenarios with various assumptions and methods (e.g. Wong et al., 2017; Le Bars et al., 2017; Stammer et al., 2019). Here, we choose to follow a consistent approach for low- and high-end scenarios, which is as follows.

- Low-end projections are based on the most conservative estimates of glaciers and ice sheet melting and stereodynamic contributions. This leads for instance to sea level rise that exceeds 0.5 m along most inhabited coastlines by 2100 under the RCP8.5 scenario (with respect to the period 1986–2005). Details on the design of these projections and the related data are published in Le Cozannet et al. (2019b).

- High-end projections are derived by considering, for each sea level component, the highest physically based modelled estimate published in the literature. For the RPC8.5 scenario, for instance, we obtain a sea level rise that exceeds 1.7 m for most of the European coastline by 2100 (with respect to the period 1986–2005). Details on the design of these projections and the related data are published in Thiéblemont et al. (2019).

Note that there is no unique approach toward high ends and low ends. If we had relied on the expert elicitation of Bamber et al. (2019), our high-end projections would have been even higher. In this study, following the approach of IPCC (Oppenheimer et al., 2019), we rely on physical modelling outcomes only.

4 Application of the framework

4.1 Analysis of past shoreline change

Past shoreline changes are investigated first to ensure the validity of the modelling framework. Table 1 summarises how uncertainties of each variable of Eq. (1) are defined (using either probability distributions or possibility distributions as introduced in Sect. 2) to model past shoreline changes in sites 1 and 2, respectively. Over the historical period, mean sea level uncertainty for these two sites is assumed to be well represented by a normal probability distribution. For vertical ground motion (VGM), the sites that are investigated in our study have no statistically significant trends identified. Therefore, uncertainties due to VGM were prescribed as a centred normal distribution with a standard deviation of $2\,\mathrm{mm\,yr^{-1}}$, as retrieved by the analysis of trends computed from the permanent coastal GNSS stations in the SONEL (Système d'Observation du Niveau des Eaux Littorales) database (Wöppelmann and Marcos, 2016). Tx and Lvar are also prescribed as normal probability distributions since they were derived assuming that errors of the linear regression are normally distributed (see Sect. 2b). Finally, as described in Sect. 2b, there is no consensus on the model to be used to project shoreline change in response to SLR. The design of the possibilistic distribution of the beach slope should therefore reflect this unknown by considering both the Bruun and the PCR model. The upper shoreface slopes are generally steeper than the nearshore slopes (e.g. 5 %–13 % versus 1 %–2 % in Aquitaine). Applying the surrogate of the PCR model leads to reduced shoreline retreat estimates in comparison with the Bruun rule estimates (see Sect. 2b). Therefore, we defined the beach slope as an imprecise parameter which follows a possibilistic trapezoid distribution that spans values ranging from the mildest records of the nearshore slope to steeper upper shoreface slopes. For site 1, this leads to a core of the trapezoid in the range 1.2 %–1.5 % and a mildest slope of 1 % (defining the origin of the support; see Table 1). For site 2, the core of the trapezoid is in the range 2 %–3.5 %, and the mildest slope is 1.5 %. Finally, in absence of a precise estimate of upper shoreface slope sites 1 and 2, we use a uniform 10 % slope as the upper point of the trapezoid (Table 1).

Figure 5 shows the lower and upper probability bounds of past ΔS for site 1 in Aquitaine and site 2 in Castellón. The results are derived from the uncertainty propagation scheme using 5000 random draws based on the uncertainty definition of each term of coastal impact model described in Table 1. For ease of comparison between the two sites, probability boxes are shown for a period of 10 years (gold) and 29–30 years (red) with respect to observational record references that are 2014 in Aquitaine and 2019 in Castellón.

For both sites, the gap between the lower and the upper bounds (i.e. the ambiguity) increases when moving increasingly backward in time (away from the reference year). This

Table 1. Chosen uncertainty representation (probabilistic or possibilistic) and data used to constrain input variables of Eq. (1). Note that Tx estimates appear slightly lower than trend estimates of Fig. 4 as the past sea level rise influence (using the Bruun rule) has been subtracted.

Variable		Chosen uncertainty representation	Value	Data source
Past sea level changes	Site 1	Probability – Gaussian	$2.3 \pm 1\,\mathrm{mm\,yr^{-1}}$ (1984–2014)	(Le Cozannet et al., 2019a)
	Site 2		$3.1 \pm 1\,\mathrm{mm\,yr^{-1}}$ (1989–2019)	Marseille's tide gauge corrected from vertical ground motion
Vertical ground motion	Site 1	Probability – Gaussian	$0 \pm 2\,\mathrm{mm\,yr^{-1}}$	Derived from Wöppelmann and Marcos (2016)
	Site 2		$0 \pm 2\,\mathrm{mm\,yr^{-1}}$	Derived from Wöppelmann and Marcos (2016)
$\tan\beta$	Site 1	Possibilistic – trapeze	[1 %, 1.2 %, 1.5 %, 10 %]	Topographic and bathymetric survey
	Site 2		[1.5 %,2 %,3.5 %,10 %]	Topographic and bathymetric survey
Lvar	Site 1	Probability – Gaussian	0 ± 7.3 m	Deduced from shoreline change observations (see Fig. 4a)
	Site 2		0 ± 5.0 m	Deduced from shoreline change observations (see Fig. 4b)
Tx	Site 1	Probability – Gaussian	$0.72 \pm 0.11\,\mathrm{mm\,yr^{-1}}$	Deduced from shoreline change observations (see Fig. 4a)
	Site 2		$0.50 \pm 0.07\,\mathrm{mm\,yr^{-1}}$	Deduced from shoreline change observations (see Fig. 4b)

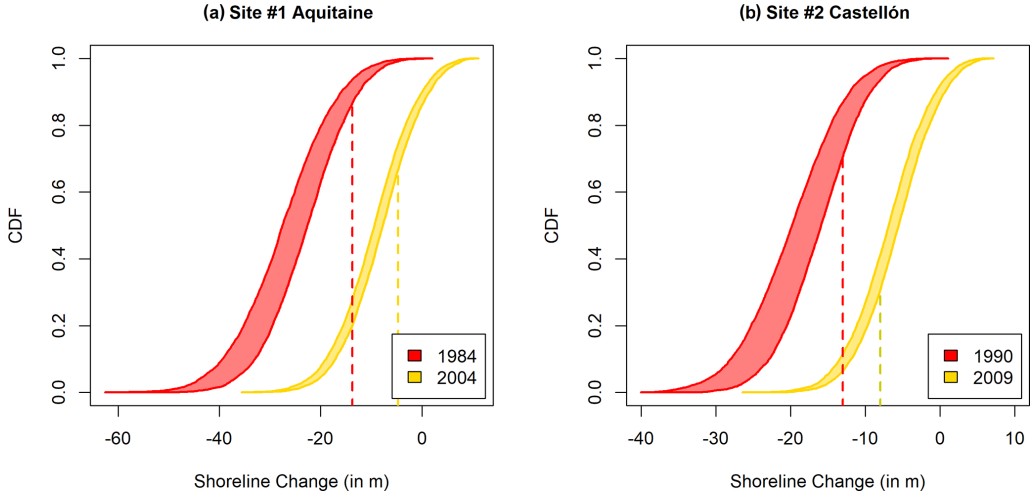

Figure 5. Past shoreline change probability boxes in **(a)** Aquitaine in 1984 and 2004 and **(b)** Castellón in 1990 and 2009, i.e. distant by 10 years (yellow) and 30 years (red) from the observational reference, respectively. The vertical dashed line indicates observed values.

is expected and simply reflects the fact that uncertainty increases when exploring them further away from the reference date. In Aquitaine, the observed anomalous shoreline position for 1984 and 2004 is −14 and −5 m, respectively (Fig. 4a). According to the associated p boxes (Fig. 5a), the probability of exceedance of these two observed values are in the ranges 86 %–92 % and 65 %–72 %, hence well embedded within possibilistic bounds but also consistent with the fact that these observations appear to be well above (especially in 1984, upper ranges) the regression estimate (Fig. 4a). In Castellón, observed shoreline positions in 1990 (2009) are −13 (−8) m, which correspond to probability of exceedance in the range 73 %–88 % (29 %–40 %). Expanding our analysis to the entire profile of site 1, we found that 55 % of the observations fall within the 25 %–75 % probability bounds and 100 % within the 5 %–95 % confidence limit. For site 2, we found that 78 % of the observations fall within the 25 %–75 % probability bounds and 96 % within the 5 %–95 % confidence limit. This hindcast analysis hence suggests that our modelling framework is valid against observational historical records.

4.2 Future projections of shoreline change

In contrast with the historical period for which observations of the mean sea level are available and its uncertainty well quantified, projections of mean sea level are deeply uncertain (see also introductory paragraph). This deep uncertainty source needs to be prescribed as input and, therefore, can no longer be considered following a normal probabilistic distribution (as shown in Table 1). The relative sea level change (RSLC) is defined as an imprecise input variable, which follows a trapezoidal possibility distribution, while all other inputs are taken identical to Table 1. We determine the RSLC possibility distribution for both time horizons 2050 and 2100 and three future climate change scenarios (RCP2.6, RCP4.5 and RCP8.5).

Table 2 gives the values of RSLR (in metres) for both time horizons and the three RCP scenarios used to construct the trapezoidal possibility distributions. The core of the trapezoid (possibility degree of 1) corresponds to the RSLR likely range as described in Sect. 3.2. For instance, for the RCP8.5 projections in 2100 with respect to 2015 (and not 1986–2005 as in IPCC), we obtain likely ranges of 0.39–0.98 m in Aquitaine and 0.47–1.03 m in Castellón, which are both lower than the global mean sea level likely range of 0.55–1.04 m. This is consistent with the results of Slangen et al. (2014) showing that North Atlantic and Mediterranean basin regional sea level projections are beneath global mean sea level estimates. The boundaries of the support of the trapezoid, to which we assign a possibility degree of 0, correspond to the low-end (lower limit) and high-end (upper limit) RSLC estimates described in Sect. 3.2.

Figure 6 shows the lower and upper probability bounds of ΔS projections for sites 1 and 2 under three future RCP scenarios. In 2050, the difference in shoreline projections and their uncertainty between future scenarios is small as shown by the median bound which extends from 25 to 49 m for RCP2.6 and 26 and 60 m for RCP8.5 in Aquitaine (Fig. 6a). This result is consistent with the fact that SLR projections start to increasingly diverge after 2050 between the three future scenarios (Garner et al., 2018; Hinkel et al., 2019). In Castellón, small inter-scenario changes are also found (Fig. 6c), but lower median bounds are under those of the Aquitaine site, i.e. $\sim$ 18 m for the Castellón site against $\sim$ 25 m for the Aquitaine site. The upper median bound is also substantially more expanded for the Aquitaine site (60 m) than the Castellón site (40 m) when considering the RCP8.5 scenario. Therefore, while scenario choice remains a modest source of uncertainty of shoreline projections by 2050, potential differences in nearshore slope and coastal impact models are already prominent. In 2100, ambiguity difference between RCP scenarios is strongly enhanced (see also Table 3). The upper uncertainty bound of the RCP8.5 scenario is more than double that of the RCP2.6 scenario in both sites.

Table 3 provides the shoreline retreat thresholds of high-end and low-end scenarios associated with the probability boxes (and thresholds a and b) displayed in Fig. 6. Although defined arbitrarily, these two thresholds represent possible – but unlikely – "optimistic" and "pessimistic" future projections that can be considered as references to design minimum adaptation and maximum protection needs, respectively. In site 1 (site 2) in 2050, whatever the scenario, it appears that the shoreline could be retreating between $\sim$ 24 m ($\sim$ 16 m) for a low-impact scenario and more than 50 m (40 m) for a high-impact scenario. High-end values strongly increase in 2100 and could reach up to almost 200 m in site 1 and more than 130 m in site 2 under the RCP8.5 scenario. Under low-end scenarios, in 2100, 58 and 37 m could still be lost in site 1 and site 2, respectively.

4.3 Sensitivity analysis

Shoreline change projections shown in Fig. 6 reveal that the uncertainty strongly amplifies with distant time horizons, in particular under high-global-warming scenarios. From a coastal planning perspective, such large uncertainties can be considered unhelpful and not be used as such to support the decision-making process (Rohmer et al., 2019). In this case, it is particularly relevant to determine which uncertainty contributes the most to the total uncertainty in order to anticipate how foreseen improvements in the understanding of the physical system could reduce the uncertainty of projections. To this end, we performed a sensitivity analysis based on the pinching method (Tucker and Ferson, 2006). The pinching method consists of quantifying how the p box changes if uncertain input parameters are pinched to a fixed value, i.e. assuming that the new knowledge context enables the removal of the corresponding epistemic uncertainty. The uncertain parameter leading to the maximum changes in the p box is the one with the largest impact, i.e. the one that deserves further investigation in priority. Here, we pinch one parameter of Eq. (1) at a time and quantify the resulting effect on the ambiguity and high-end values.

Figure 7 shows the results of the sensitivity analysis applied to site 1 for the RCP8.5 scenario in 2100. Note that this analysis has been extended to all scenarios and site 2 and revealed close results, leading to similar conclusions. The figure reads as follows: assuming that the sea level off the Aquitaine coast would rise by 0.37 m in 2100 only (a very low estimate), the ambiguity (Fig. 7a) and high-end estimate (Fig. 7b) of shoreline change projection would both reduce by more than 50 %. These results show that ambiguity and high-end estimate are primarily sensitive to uncertainty in SLR and beach slope. Ambiguity and high-end estimate in shoreline change projections increase linearly with increasing SLR and decrease more abruptly (following an inverse function, consistent with Eq. 1) with increasing beach slope. In comparison, the Tx and Lvar uncertainties have practically no effect on the ambiguity of shoreline change projections but show some influence on high-end estimates. The high-

Table 2. RSLR (in metres) projections in Aquitaine and Castellón for the RCP2.6, RCP4.5 and RCP8.5 scenarios in 2050 and 2100. RSLC projections are expressed as changes with respect to the year 2015. The first and fourth values in brackets correspond to RSLC estimates that define the support of the trapezoid (associated with a possibility degree of 0), and the second and third values in brackets correspond to RSLC estimates that define the core of the trapezoid (associated with a possibility degree of 1).

	RCP2.6		RCP4.5		RCP8.5	
	Aquitaine	Castellón	Aquitaine	Castellón	Aquitaine	Castellón
2050	[0.02, 0.06, 0.22, 0.31]	[0.07, 0.10, 0.23, 0.30]	[0.05, 0.06, 0.24, 0.39]	[0.09, 0.11, 0.24, 0.38]	[0.06, 0.08, 0.27, 0.50]	[0.09, 0.12, 0.28, 0.50]
2100	[0.08, 0.12, 0.48, 0.72]	[0.13, 0.19, 0.52, 0.72]	[0.19, 0.20, 0.57, 1.11]	[0.23, 0.26, 0.62, 1.16]	[0.37, 0.39, 0.98, 1.82]	[0.44, 0.47, 1.03, 1.83]

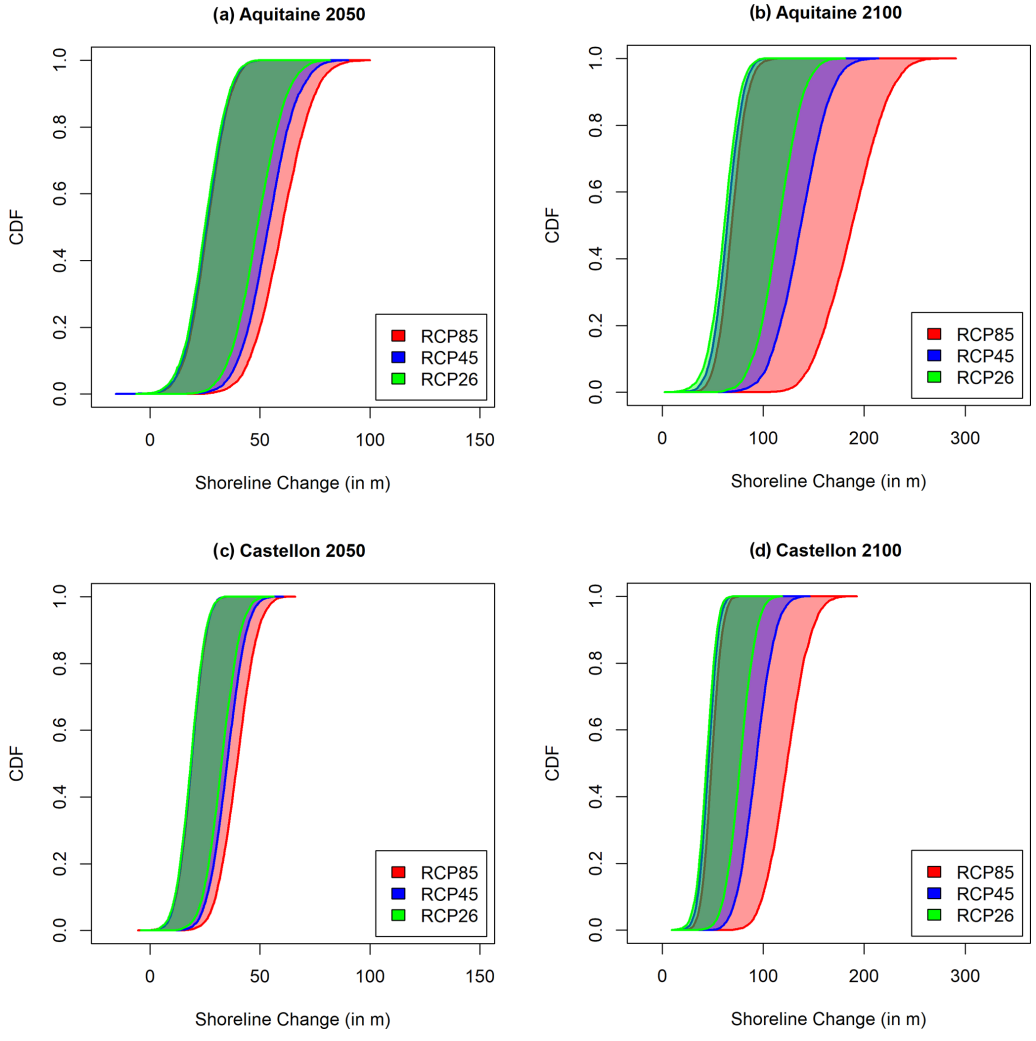

Figure 6. Projected shoreline change probability boxes in **(a, c)** 2050 and **(b, d)** 2100 for **(a, b)** site 1 in Aquitaine and **(c, d)** site 2 in Castellón. Projections are shown for the (green) RCP2.6, (blue) RCP4.5 and (red) RCP8.5 scenarios. Ambiguity and low- and high-end corresponding values are given in Table 3.

Table 3. Ambiguity and low- and high-end projected shoreline change thresholds [in metres] in 2050 and 2100 for site 1 in Aquitaine and site 2 in Castellón. Green, blue and red numbers indicate thresholds for the RCP2.6, RCP4.5 and RCP8.5 scenarios, respectively.

	Site 1 2050	Site 1 2100	Site 2 2050	Site 2 2100
Ambiguity [m]	24/28/34	54/73/119	14/16/21	34/47/75
Low-end [m]	23/23/24	58/61/66	15/16/16	37/39/42
High-end [m]	52/57/63	120/144/196	35/38/43	85/100/132

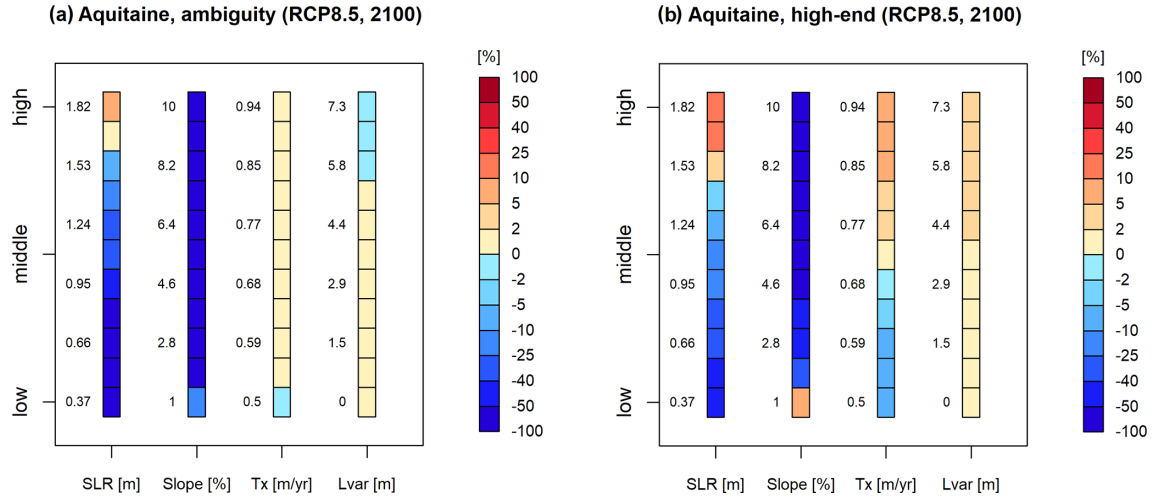

Figure 7. Relative change (in percent) of the p-box ambiguity **(a)** and high-end estimate **(b)** when the possibility (or probability) input distribution of one of the terms in Eq. (1) (i.e. SLR, Tx) is pinched to a fixed value. For each term, 11 values are pinched at a regular interval from the lower to the upper range of the possibility (or probability) distribution. These pinched values are specified on the left side of each bar plot. Site 1 is shown.

end shoreline change sensitivity to Tx and Lvar is also more pronounced in 2050 (not shown).

Interestingly, we note that the ambiguity increases when fixing SLR to high values (i.e. greater than 1.6 m, Fig. 7a). Intuitively, we expect the ambiguity to decrease when additional knowledge is provided, i.e. when the epistemic uncertainty is decreased. Yet, this holds only if the IRS-based randomly generated intervals (see step 3 in Appendix A) are of lower widths given the fixed value. This is not always the case and depends on the characteristics (like the monotony) of the mathematical function optimised at step 3 (given the fixed value). Figure S1 in the Supplement illustrates this effect by comparing the p boxes for the case where the full SLR possibility distribution is considered against the case where the SLR value is fixed to 1.82 m. The p box of the latter case shows an overall shift of the lower and upper CDFs to higher values and a change in the width between the lower and upper CDFs.

This sensitivity analysis therefore suggests that improving both SLR projections and the understanding of their impact on shoreline could lead to a substantial reduction of uncertainty of future shoreline change. It should be emphasised that in the event that future SLR would not exceed the likely range (i.e. ~ 1 m), the ambiguity would be lowered by more than 50 %. Similarly, knowing the nearshore slope exactly contributes to drastically reduce the shoreline change uncertainty, in particular if this nearshore slope is steep (i.e. > 2 %). Fixing the beach slope value in our simplified shoreline change equation implicitly suggests, though, that the coastal impact model is also well defined. The latter underlying assumption is however erroneous as reviewed previously (e.g. Sect. 2.2). In the discussion, we explore in more detail how shoreline change uncertainty is sensitive to the coastal impact model.

5 Discussion

5.1 Bruun vs. surrogate PCR model

By opting for a trapezoidal possibility distribution to represent the deep uncertainty on the nearshore slope as input of our shoreline change model, we recognise that the coastal impact is not well constrained since we assume together the Bruun rule and the surrogate PCR model within a single

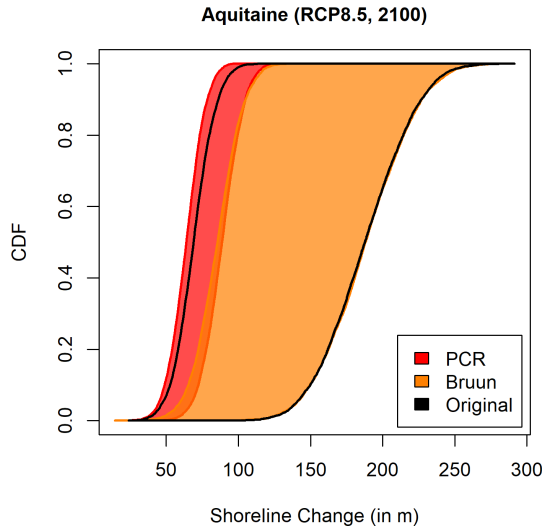

Figure 8. Projected shoreline change p box in 2100 for site 1 under the RCP8.5 scenario. The reference model is displayed with the black envelop, and the modified models following the PCR model emulation and Bruun rule, are displayed in red and orange, respectively.

trapezoidal possibility distribution. We actually may wonder what would imply an improved knowledge of coastal impact models on shoreline change projections. In other words, how is the ambiguity affected if either the surrogate PCR model or the Bruun rule is excluded?

To address this question, we have changed the nearshore slope definition as input of our model. Results are shown in Fig. 8. To consider solely the Bruun model, beach slopes are defined as trapezoidal considering the range 1.2 %–1.5 % for the core and 1 %–1.6 % for the support. Note that the 1.2 % and 1.5 % beach slopes correspond to the interval of foreshore slope from the dune toe to the depth of closure in Aquitaine (i.e. Bruun slopes). For the PCR model emulation, we adopted the approach of Le Cozannet et al. (2019a), where the slopes of the upper shoreface are substituted to the Bruun slopes. In site 1, slopes of the upper shoreface are comprised between 5 % and 13 %. Therefore, the PCR model was emulated by defining beach slopes as trapezoidal considering the core 5.1 %–12.9 % and the support 5 %–13 %.

In Fig. 8, the PCR model emulation (red) and Bruun model (orange) realisations are compared to the reference model (black p-box envelop). Our results reveal that the Bruun model fits the upper bound of the reference model nicely and encompasses most of the ambiguity. In contrast, the p box built from the PCR emulation model overlaps the reference model in its lower bounds and has an area 4 times smaller than for the Bruun model. Therefore, considering the PCR model leads to a strong reduction of the uncertainty of SLR-induced shoreline change but also to a sharp decrease in projected coastline retreat. This is due to the fact that the SLR-induced shoreline change is proportional to the inverse of the beach slope, which varies weakly on the range of beach slopes 5 %–13 %. Conversely, the Bruun model exacerbates shoreline change ambiguity and shoreline change sensitivity to SLR uncertainties.

5.2 Considering anthropisation

Along the Castellón coastal stretch, most sectors have been affected by human intervention. This implies that great caution is needed when applying our simple shoreline change model for this area. For instance, in Almardà (south of Chilches), beach nourishments have been carried out over the 1995–1998 and 2010–2013 periods, resulting in an overall beach accretion of 1.5 m yr^{-1} over the 1989–2019 period as shown in Fig. 9a. Outside beach nourishment periods though, shoreline retreat is observed as revealed by a positive trend displayed in red. Although our shoreline change model does not explicitly include past anthropogenic influences, effects such as beach nourishment can be implicitly accounted for in the Tx and Lvar terms. For instance, for Almardà (Fig. 9a), the Tx is negative (i.e. beach accretion) due to beach nourishment. Therefore, shoreline change projections made for this site would assume that beach nourishment will be pursued in the future at the same rates and frequency. In such a case, our projections show that by 2100 and even under RCP8.5, shoreline is expected to further progress toward the sea, with a very large uncertainty though as revealed by the black p box in Fig. 9b.

Assuming that beach nourishment will continue is however strongly uncertain and should be avoided. In this regard, we derived the Tx term by relying only on periods outside beach nourishment shown by the red segments. This leads to a weighted mean Tx of 0.83 m yr^{-1}. The resulting projections in 2100 under the RCP8.5 scenario are shown by the red p box, which in this case clearly indicates that in absence of future beach nourishment, the shoreline is projected to retreat in the face of sea level rise. The ambiguity remains very similar, indicating that accounting for beach nourishment simply translates the p box. Nonetheless, we note that when the nourishment is not included, the p box is more tilted, which is due to the higher standard error associated with the Tx term.

5.3 Advantages of extra-probabilistic approaches

Here, we discuss the advantage of the use of possibilities in comparison to a modelling framework that would be fully probabilistic. To illustrate this, we re-calculate shoreline change projections with Eq. (1) in Aquitaine (site 1) in 2100 but assuming that ΔRSLC and $\tan\beta$ follow normal distributions. We consider the RCP8.5 scenario with ΔRSLC defined as $0.69\,\text{m} \pm 0.24\,\text{m}$ and the Bruun rule with $\tan\beta$ defined as $1.35\,\% \pm 0.15\,\%$. The resulting shoreline change projections are normally distributed with 5th and 95th percentiles of 71 and 152 m, respectively. Within a probabilis-

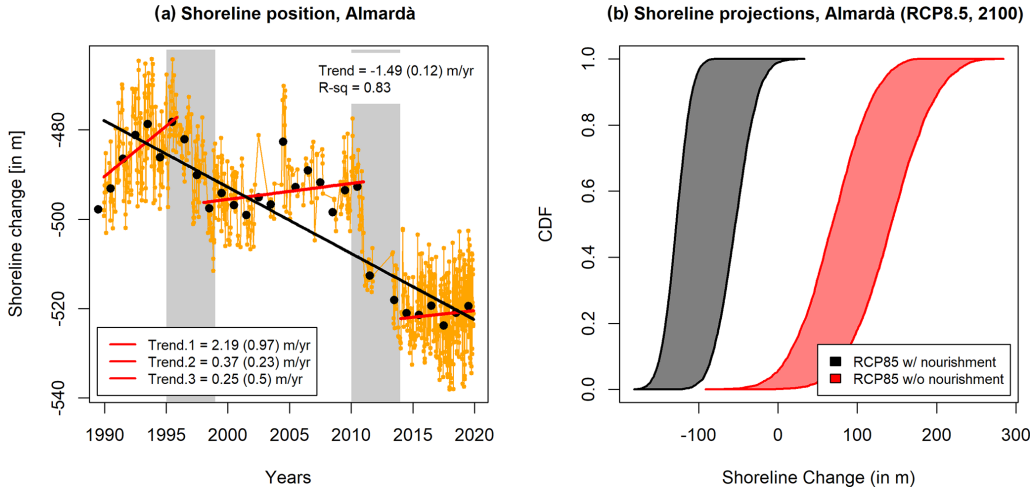

Figure 9. (a) Observed shoreline change evolution in Almardà. The black and red lines indicate trends computed with and without, respectively, the periods of beach nourishment, which are displayed in grey. **(b)** Probability boxes of projected shoreline change by 2100 under the RCP8.5 scenarios with (black) and without (red) including beach nourishment.

tic approach, these left and right tails can be reasonably associated with low- and high-end projections. The comparison with extra-probabilistic low- and high-end projections in Table 3 (i.e. 66 and 196 m, respectively) shows substantial differences and in particular that high-end values obtained within the probabilistic theory are much lower. More importantly, we found that the high-end projection obtained with the possibilistic framework is not even achievable under the probabilistic model built here, hence indicating that the probability-based high-end scenario is too optimistic in the sense that it fails to reflect deep uncertainty. One should thus design dedicated (and separated) high-end scenarios to explore such projections that may appear arbitrary.

Another strength of the extra-probabilistic framework is its flexibility with respect to the available expert data, which allows easily fusing different low- and high-end scenarios. In this study, we accounted for the deep uncertainty in future SLR by designing RSLC projections that follow a trapezoid possibility function and selecting a set of low- and high-end estimates to bound the support of the trapezoid. As mentioned in Sect. 3.2, there is no unique approach to design low- and high-end projections yet. Possibility functions can therefore be adapted to encompass multiple high-end estimates. For instance Le Cozannet et al. (2017) translated expert opinions on future Antarctica contribution into three different possible upper bounds for 2100 sea level rise. These estimates were then aggregated into a single stair-like input function where the three high-end scenarios were assigned various degrees of possibility. Applying this aggregated possibility distribution in our case would result in similar ambiguity estimates but with an increase in the p box's upper tail (for percentile superior to 90 %) up to values of 500 m (by 2100 for Aquitaine; see Fig. S2 in the Supplement).

Finally, the problem of model uncertainty related to the use of the Bruun or the surrogate PCR model provides a good illustration of how the quantified measure of ambiguity in the projection can de decomposed. The use of possibilities allows us to make the ambiguity very transparent thanks to the p boxes' graphical representation. This also has the advantage of showing how future progress in the system knowledge may contribute to reducing deep uncertainty. From a decision-making perspective, the extra-probabilistic approach thus allows a transparent and exhaustive consideration of uncertainties. One should nonetheless bear in mind that in case knowledge uncertainty becomes very prominent and requires an extensive use of possibility distribution as input, the ambiguity in the outcome may be considered by end-users to be too large to be informative and useful.

6 Conclusion

The approach presented in this paper provides a framework for assessing deep uncertainties in shoreline change projections. This framework is versatile since the definition of input variables and their distribution can be adapted easily to the characteristics of a local site, its data coverage and the degree of knowledge of hydrosedimentary processes acting locally. Furthermore, this extra-probabilistic approach that we here apply to an empirical shoreline evolution model can actually be replicated for any of the available models of shoreline evolution (Montaño et al., 2020).

In our approach, residual uncertainties that have not been integrated quantitatively still remain. For example, the Bruun rule and the PCR models are not the only plausible models for shoreline change reconstructions. Similarly, our high-end sea level rise estimates might be exceeded by 2050 accord-

ing to recent expert elicitation of the future contribution of Greenland and Antarctica ice sheets to sea level rise (Bamber et al., 2019). The approach consisting in summing up the different modes of variability of shoreline change can also be challenged on the ground. For example, coastal defences may limit the potential retreat of shorelines in other areas. Finally, future adaptation is unknown and could limit or favour coastal erosion and shoreline changes.

Despite these limitations, our approach is potentially useful to determine to which extent reducing our uncertainties on future sea level rise or coastal impact models can help improve the precision of future shoreline change projections. For example, we have shown that if sea level rise does not exceed 1 m, shoreline change uncertainties will be reduced significantly. This could be achieved through an ambitious climate mitigation policy and improved knowledge on ice sheets. While there remains the issue of the long-term commitment to sea level rise (Clark et al., 2016), reducing this source of deep uncertainties would grant more time for coastal adaptation.

Appendix A: The independent random sampling (IRS) algorithm

Consider k random input variables X_i $(i = 1, \ldots, k)$, each of them associated with a cumulative probability distribution F, and $n-k$ imprecise input variables X_i $(i = k+1, \ldots, n)$, each of them associated with a possibility distribution π. In this situation, the IRS procedure holds as follows.

- Step 1. Randomly generate m vectors of size n from uniform probability distributions: $\{\alpha_i\}, i = 1, \ldots, n$, such that $0 \leq \alpha_i \leq 1$. For each realisation, perform the following.
- Step 2. Generate k values for the random input variables by using the inverse function of F_i: $x_i = F_i^{-1}(\alpha_i)$, $i = 1, \ldots, k$ and sample $n-k$ intervals I_i corresponding to the cuts of the possibility distributions (as defined in Sect. 2.1 and illustrated in Fig. 1) with a level of confidence $1-\alpha_i$, $i = k+1, \ldots, n$.
- Step 3. Evaluate the interval $[\underline{h}; \overline{h}]$ defined by the lower and upper bounds associated with the model output h (in our case, the shoreline change) using the impact assessment model f as follows:

$$\underline{h} = \inf\left(f\left(x_1; \ldots; x_k; I_{k+1}; \ldots; I_n\right)\right);$$
$$\overline{h} = \inf\left(f\left(x_1; \ldots; x_k; I_{k+1}; \ldots; I_n\right)\right).$$

Figure A1 schematically depicts the main steps of the propagation procedure considering a random and an imprecise variable. The output of the whole procedure then takes the form of m random intervals $[\underline{h}; \overline{h}]$, with $k = 1, \ldots, m$. This information can be summarised within the formal framework of the evidence theory (Dempster, 1967; Shafer, 1976) as proposed by Baudrit et al. (2005) to bound the exceedance probability associated with the event "$h \geq t_h$" with t_h a given threshold. The result then takes the form of the probability boxes as depicted in Fig. 5.

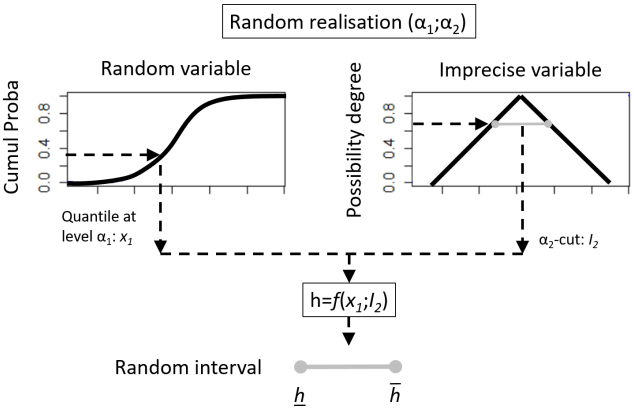

Figure A1. Overview of the main steps for joint propagation of possibility and probability distributions. Adapted from Rohmer and Verdel (2014).

Code availability. HYRISK software, used to design and jointly propagate probability and possibility distributions is a publicly available CRAN R package (https://cran.r-project.org/web/packages/HYRISK/index.html; Rohmer et al., 2021). R code and data needed to reproduce simulations, shoreline reconstructions and projections, and related figures for each case study are publicly available at https://gitlab.brgm.fr/brgm/shoreline-change-hyrisk (BRGM, 2021a).

Data availability. AR5 projections can be downloaded from the Integrated Climate Data Center at the University of Hamburg (https://icdc.cen.uni-hamburg.de/en/ar5-slr.html; University of Hamburg, 2021). Other projections (i.e. low-end, high-end projections) used in this study are available at https://sealevelrise.brgm.fr/ (BRGM, 2021b). Other data such as shoreline observations used in this paper will be made available with the code.

Supplement. The supplement related to this article is available online at: https://doi.org/10.5194/nhess-21-2257-2021-supplement.

Author contributions. RT designed the sea level projections and performed the data analysis and the simulations. GL had the original idea of the study and contributed to the design and to the interpretation of the simulations. JR developed the HYRISK software used to perform the simulations and participated in their interpretation. AT, MAC and IJL retrieved the shoreline data in Castellón and contributed to interpretation of their projections. RT prepared the manuscript with contributions from all co-authors.

Competing interests. The authors declare that they have no conflict of interest.

Disclaimer. Publisher's note: Copernicus Publications remains neutral with regard to jurisdictional claims in published maps and institutional affiliations.

Acknowledgements. This research takes part in the COasTAUD framework. We thank Mark Carson for making available the ICDC sea level data and the modelling groups that participated in the CMIP5 for producing their model output. We also thank SONEL and PSMSL services for providing tide gauges and GPS land motion records. We thank Bruno Castelle for providing the shoreline change historical evolution dataset in Aquitaine. We thank the two anonymous reviewers for their constructive comments on our work.

Financial support. This research has been supported by the BRGM, IHCantabria and the ERA4CS-ECLISEA project (grant no. 690462).

Review statement. This paper was edited by Ira Didenkulova and reviewed by two anonymous referees.

References

Athanasiou, P., van Dongeren, A., Giardino, A., Vousdoukas, M. I., Ranasinghe, R., and Kwadijk, J.: Uncertainties in projections of sandy beach erosion due to sea level rise: an analysis at the European scale, Sci. Rep., 10, 11895, https://doi.org/10.1038/s41598-020-68576-0, 2020.

Bakker, A. M. R., Louchard, D., and Keller, K.: Sources and implications of deep uncertainties surrounding sea-level projections, Clim. Change, 140, 339–347, https://doi.org/10.1007/s10584-016-1864-1, 2017.

Bamber, J. L., Oppenheimer, M., Kopp, R. E., Aspinall, W. P., and Cooke, R. M.: Ice sheet contributions to future sea-level rise from structured expert judgment, Proc. Natl. Acad. Sci. USA, 116, 11195, https://doi.org/10.1073/pnas.1817205116, 2019.

Baudrit, C., Guyonnet, D., and Dubois, D.: Postprocessing the Hybrid Method for Addressing Uncertainty in Risk Assessments, J. Environ. Eng., 131, 1750–1754, https://doi.org/10.1061/(ASCE)0733-9372(2005)131:12(1750), 2005.

Baudrit, C., Guyonnet, D., and Dubois, D.: Joint propagation of variability and imprecision in assessing the risk of groundwater contamination, J. Contam. Hydrol., 93, 72–84, https://doi.org/10.1016/j.jconhyd.2007.01.015, 2007.

Beer, M., Ferson, S., and Kreinovich, V.: Imprecise probabilities in engineering analyses, Mech. Syst. Signal Pr., 37, 4–29, https://doi.org/10.1016/j.ymssp.2013.01.024, 2013.

Bernon, N., Mallet, C., and Belon, R.: Caractérisation de l'aléa recul du trait de côte sur le littoral de la côte aquitaine aux horizons 2025 et 2050, Rapport final, BRGM/RP-66277-FR, 99 pp., available at: https://www.actu-environnement.com/media/pdf/news-28220-littoral-aquitain-recul.pdf (last access: 29 June 2021), 2016.

Beven, K. J., Almeida, S., Aspinall, W. P., Bates, P. D., Blazkova, S., Borgomeo, E., Freer, J., Goda, K., Hall, J. W., Phillips, J. C., Simpson, M., Smith, P. J., Stephenson, D. B., Wagener, T., Watson, M., and Wilkins, K. L.: Epistemic uncertainties and natural hazard risk assessment – Part 1: A review of different natural hazard areas, Nat. Hazards Earth Syst. Sci., 18, 2741–2768, https://doi.org/10.5194/nhess-18-2741-2018, 2018.

BRGM: Shoreline change Hyrisk Gitlab, available at: https://gitlab.brgm.fr/brgm/shoreline-change-hyrisk, last access: 29 July 2021a.

BRGM: Regional sea level changes, available at: https://sealevelrise.brgm.fr/sea-level-scenarios, last access: 22 June 2021b.

Bruun, P.: Sea-Level Rise as a Cause of Shore Erosion, Journal of the Waterways and Harbors Division, 88, 117–132, 1962.

Budescu, D. V., Broomell, S. B., Lempert, R. J., and Keller, K.: Aided and unaided decisions with imprecise probabilities in the domain of losses, EURO Journal on Decision Processes, 2, 31–62, https://doi.org/10.1007/s40070-013-0023-4, 2014.

Bulteau, T., Mugica, J., Mallet, C., Garnier, C., Rosebery, D., Maugard, F., Nicolae Lerma , A., and Naho, A.: Évaluation de l'impact des tempêtes de l'hiver 2013–2014 sur la morphologie

de la Côte Aquitaine, Rapport final, BRGM/RP-63797-FR, 68 pp., 138, fig., 8 tab., 2 ann., 2014.

Carson, M., Kohl, A., Stammer, D., Slangen, A. B. A., Katsman, C. A., van de Wal, R. S. W., Church, J., and White, N.: Coastal sea level changes, observed and projected during the 20th and 21st century, Clim. Change, 134, 269–281, https://doi.org/10.1007/s10584-015-1520-1, 2016.

Castelle, B., Guillot, B., Marieu, V., Chaumillon, E., Hanquiez, V., Bujan, S., and Poppeschi, C.: Spatial and temporal patterns of shoreline change of a 280 km high-energy disrupted sandy coast from 1950 to 2014: SW France, Estuar. Coast. Shelf S., 200, 212–223, https://doi.org/10.1016/j.ecss.2017.11.005, 2018.

Church, J. A., Clark, P. U., Cazenave, A., Gregory, J. M., Jevrejeva, S., Levermann, A., Merrifield, M. A., Milne, G. A., Nerem, R. S., Nunn, P. D., Payne, A. J., Pfeffer, W. T., Stammer, D., and Unnikrishnan, A. S.: Sea Level Change, in: Climate Change 2013: The Physical Science Basis. Contribution of Working Group I to the Fifth Assessment Report of the Intergovernmental Panel on Climate Change ed., Cambridge University Press, Cambridge, United Kingdom and New York, NY, USA, 2013.

Clark, P. U., Shakun, J. D., Marcott, S. A., Mix, A. C., Eby, M., Kulp, S., Levermann, A., Milne, G. A., Pfister, P. L., Santer, B. D., Schrag, D. P., Solomon, S., Stocker, T. F., Strauss, B. H., Weaver, A. J., Winkelmann, R., Archer, D., Bard, E., Goldner, A., Lambeck, K., Pierrehumbert, R. T., and Plattner, G. K.: Consequences of twenty-first-century policy for multi-millennial climate and sea-level change, Nat. Clim. Change, 6, 360–369, https://doi.org/10.1038/nclimate2923, 2016.

Cooper, J. A. G. and Pilkey, O. H.: Sea-level rise and shoreline retreat: time to abandon the Bruun Rule, Global Planet. Change, 43, 157–171, https://doi.org/10.1016/j.gloplacha.2004.07.001, 2004.

Cooper, J. A. G., Masselink, G., Coco, G., Short, A. D., Castelle, B., Rogers, K., Anthony, E., Green, A. N., Kelley, J. T., Pilkey, O. H., and Jackson, D. W. T.: Sandy beaches can survive sea-level rise, Nat. Clim. Change, 10, 993–995, https://doi.org/10.1038/s41558-020-00934-2, 2020.

Cowell, P. J., Stive, M. J. F., Niedoroda, A. W., de Vriend, H. J., Swift, D. J. P., Kaminsky, G. M., and Capobianco, M.: The Coastal-Tract (Part 1): A Conceptual Approach to Aggregated Modeling of Low-Order Coastal Change, J. Coastal Res., 19, 812–827, 2003.

DeConto, R. M. and Pollard, D.: Contribution of Antarctica to past and future sea-level rise, Nature, 531, 591–597, 2016.

Dempster, A. P.: Upper and lower probabilities induced by a multivalued mapping, Ann. Math. Stat., 38, 325–339, 1967.

Dubois, D. and Guyonnet, D.: Risk-informed decision-making in the presence of epistemic uncertainty, International Journal of General Systems, 40, 145-167, https://doi.org/10.1080/03081079.2010.506179, 2011.

Dubois, D. and Prade, H.: Possibility Theory: An Approach to Computerized Processing of Uncertainty, Plenum Press, New York, 1988.

Dubois, D. and Prade, H.: On the Combination of Evidence in Various Mathematical Frameworks, in: Reliability Data Collection and Analysis, edited by: Flamm, J. and Luisi, T., Springer the Netherlands, Dordrecht, 213–241, 1992.

Edwards, T. L., Brandon, M. A., Durand, G., Edwards, N. R., Golledge, N. R., Holden, P. B., Nias, I. J., Payne, A. J., Ritz, C., and Wernecke, A.: Revisiting Antarctic ice loss due to marine ice-cliff instability, Nature, 566, 58–64, https://doi.org/10.1038/s41586-019-0901-4, 2019.

Enríquez, A. R., Marcos, M., Falqués, A., and Roelvink, D.: Assessing Beach and Dune Erosion and Vulnerability Under Sea Level Rise: A Case Study in the Mediterranean Sea, Frontiers in Marine Science, 6, 4, https://doi.org/10.3389/fmars.2019.00004, 2019.

Garner, A. J., Weiss, J. L., Parris, A., Kopp, R. E., Horton, R. M., Overpeck, J. T., and Horton, B. P.: Evolution of 21st Century Sea Level Rise Projections, Earths Future, 6, 1603–1615, https://doi.org/10.1029/2018ef000991, 2018.

Gregory, J. M., Griffies, S. M., Hughes, C. W., Lowe, J. A., Church, J. A., Fukimori, I., Gomez, N., Kopp, R. E., Landerer, F., Le Cozannet, G., Ponte, R. M., Stammer, D., Tamisiea, M. E., and van de Wal, R. S. W.: Concepts and Terminology for Sea Level: Mean, Variability and Change, Both Local and Global, Surv. Geophys., 40, 1251–1289, https://doi.org/10.1007/s10712-019-09525-z, 2019.

Helgeson, C., Srikrishnan, V., Keller, K., and Tuana, N.: Why Simpler Computer Simulation Models Can Be Epistemically Better for Informing Decisions, Philos. Sci., 88, 213–233, https://doi.org/10.1086/711501, 2020.

Hinkel, J., Jaeger, C., Nicholls, R. J., Lowe, J., Renn, O., and Shi, P. J.: Sea-level rise scenarios and coastal risk management, Nat. Clim. Change, 5, 188–190, https://doi.org/10.1038/nclimate2505, 2015.

Hinkel, J., Church, J. A., Gregory, J. M., Lambert, E., Le Cozannet, G., Lowe, J., McInnes, K. L., Nicholls, R. J., van der Pol, T. D., and van de Wal, R.: Meeting User Needs for Sea Level Rise Information: A Decision Analysis Perspective, Earths Future, 7, 320–337, https://doi.org/10.1029/2018ef001071, 2019.

Joughin, I., Smith, B. E., and Medley, B.: Marine Ice Sheet Collapse Potentially Under Way for the Thwaites Glacier Basin, West Antarctica, Science, 344, 735, https://doi.org/10.1126/science.1249055, 2014.

Kopp, R. E., DeConto, R. M., Bader, D. A., Hay, C. C., Horton, R. M., Kulp, S., Oppenheimer, M., Pollard, D., and Strauss, B. H.: Evolving Understanding of Antarctic Ice-Sheet Physics and Ambiguity in Probabilistic Sea-Level Projections, Earths Future, 5, 1217–1233, https://doi.org/10.1002/2017ef000663, 2017.

Le Bars, D., Drijfhout, S., and de Vries, H.: A high-end sea level rise probabilistic projections includiing rapid Antarctic ice sheet mass loss, Environ. Res. Lett., 12, 044013, https://doi.org/10.1088/1748-9326/aa6512, 2017.

Le Cozannet, G., Manceau, J. C., and Rohmer, J.: Bounding probabilistic sea-level projections within the framework of the possibility theory, Environ. Res. Lett., 12, 014012, https://doi.org/10.1088/1748-9326/aa5528, 2017.

Le Cozannet, G., Bulteau, T., Castelle, B., Ranasinghe, R., Woppelmann, G., Rohmer, J., Bernon, N., Idier, D., Louisor, J., and Salas-y-Melia, D.: Quantifying uncertainties of sandy shoreline change projections as sea level rises, Sci. Rep., 9, 42, https://doi.org/10.1038/s41598-018-37017-4, 2019a.

Le Cozannet, G., Thiéblemont, R., Rohmer, J., Idier, D., Manceau, J.-C., and Quique, R.: Low-End Probabilistic Sea-Level Projections, Water, 11, 1507, https://doi.org/10.3390/w11071507, 2019b.

Luijendijk, A., Hagenaars, G., Ranasinghe, R., Baart, F., Donchyts, G., and Aarninkhof, S.: The State of the World's Beaches, Sci. Rep., 8, 6641, https://doi.org/10.1038/s41598-018-24630-6, 2018.

Marcos, M. and Tsimplis, M. N.: Coastal sea level trends in Southern Europe, Geophys. J. Int., 175, 70–82, https://doi.org/10.1111/j.1365-246X.2008.03892.x, 2008.

Mentaschi, L., Vousdoukas, M. I., Pekel, J. F., Voukouvalas, E., and Feyen, L.: Global long-term observations of coastal erosion and accretion, Sci. Rep., 8, 12876, https://doi.org/10.1038/s41598-018-30904-w, 2018.

Montaño, J., Coco, G., Antolínez, J. A. A., Beuzen, T., Bryan, K. R., Cagigal, L., Castelle, B., Davidson, M. A., Goldstein, E. B., Ibaceta, R., Idier, D., Ludka, B. C., Masoud-Ansari, S., Méndez, F. J., Murray, A. B., Plant, N. G., Ratliff, K. M., Robinet, A., Rueda, A., Sénéchal, N., Simmons, J. A., Splinter, K. D., Stephens, S., Townend, I., Vitousek, S., and Vos, K.: Blind testing of shoreline evolution models, Sci. Rep., 10, 2137, https://doi.org/10.1038/s41598-020-59018-y, 2020.

Nicholls, R. J., Hanson, S. E., Lowe, J. A., Warrick, R. A., Lu, X. F., and Long, A. J.: Sea-level scenarios for evaluating coastal impacts, WiRes Clim. Change, 5, 129–150, https://doi.org/10.1002/wcc.253, 2014.

Oppenheimer, M., Glavovic, B. C., Hinkel, J., van de Wal, R., Magnan, A. K., Abd-EIgawad, A., Cai, R., Cifuentes-Jara, M., DeConto, R. M., Ghosh, T., Hay, J., Isla, F., Marzeion, B., Meyssignac, B., and Sebesvari, Z.: Sea level rise and implications for low-Lying islands, coasts and communities, in: IPCC Special Report on the Ocean and Cryosphere in a Changing Climate, edited by: Pörtner, H.-O., et al., Cambridge University Press, 2019.

Peter, J. C., Marcel, J. F. S., Alan, W. N., Huib, J. d. V., Donald, J. P. S., George, M. K., and Michele, C.: The Coastal-Tract (Part 1): A Conceptual Approach to Aggregated Modeling of Low-Order Coastal Change, J. Coastal Res., 19, 812–827, 2003.

Ranasinghe, R.: Assessing climate change impacts on open sandy coasts: A review, Earth-Sci. Rev., 160, 320–332, https://doi.org/10.1016/j.earscirev.2016.07.011, 2016.

Ranasinghe, R.: On the need for a new generation of coastal change models for the 21st century, Sci. Rep., 10, 2010, https://doi.org/10.1038/s41598-020-58376-x, 2020.

Ranasinghe, R. and Stive, M. J. F.: Rising seas and retreating coastlines, Clim. Change, 97, 465, https://doi.org/10.1007/s10584-009-9593-3, 2009.

Ranasinghe, R., Callaghan, D., and Stive, M. J. F.: Estimating coastal recession due to sea level rise: beyond the Bruun rule, Clim. Change, 110, 561–574, https://doi.org/10.1007/s10584-011-0107-8, 2012.

Rignot, E., Mouginot, J., Morlighem, M., Seroussi, H., and Scheuchl, B.: Widespread, rapid grounding line retreat of Pine Island, Thwaites, Smith, and Kohler glaciers, West Antarctica, from 1992 to 2011, Geophys. Res. Lett., 41, 3502–3509, https://doi.org/10.1002/2014GL060140, 2014.

Robinet, A., Idier, D., Castelle, B., and Marieu, V.: A reduced-complexity shoreline change model combining longshore and cross-shore processes: The LX-Shore model, Environ. Modell. Softw., 109, 1–16, https://doi.org/10.1016/j.envsoft.2018.08.010, 2018.

Rohmer, J. and Verdel, T.: Joint exploration of regional importance of possibilistic and probabilistic uncertainty in stability analysis, Comput. Geotech., 61, 308–315, https://doi.org/10.1016/j.compgeo.2014.05.015, 2014.

Rohmer, J., Manceau, J., Guyonnet, D., and Boulahya, F.: HYRISK: Hybrid Methods for Addressing Uncertainty in RISK Assessments, Eartharxiv, https://doi.org/10.31223/osf.io/j67cy, 2018.

Rohmer, J., Le Cozannet, G., and Manceau, J.-C.: Addressing ambiguity in probabilistic assessments of future coastal flooding using possibility distributions, Clim. Change, 155, 95–109, https://doi.org/10.1007/s10584-019-02443-4, 2019.

Rohmer, J., Manceau, J.-C., Guyonnet, D., and Boulahya, F.: HYRISK: Hybrid Methods for Addressing Uncertainty in RISK Assessments, available at: https://cran.r-project.org/web/packages/HYRISK/index.html, last access: 22 June 2021.

Shafer, G.: A mathematical theory of evidence, B. Lond. Math. Soc., 9, 237–238, 1976.

Slangen, A. B. A., Katsman, C. A., van de Wal, R. S. W., Vermeersen, L. L. A., and Riva, R. E. M.: Towards regional projections of twenty-first century sea-level change based on IPCC SRES scenarios, Clim. Dynam., 38, 1191–1209, https://doi.org/10.1007/s00382-011-1057-6, 2012.

Slangen, A. B. A., Carson, M., Katsman, C. A., van de Wal, R. S. W., Kohl, A., Vermeersen, L. L. A., and Stammer, D.: Projecting twenty-first century regional sea-level changes, Clim. Change, 124, 317–332, https://doi.org/10.1007/s10584-014-1080-9, 2014.

Slangen, A. B. A., Adloff, F., Jevrejeva, S., Leclercq, P. W., Marzeion, B., Wada, Y., and Winkelmann, R.: A Review of Recent Updates of Sea-Level Projections at Global and Regional Scales, Surv. Geophys., 38, 385–406, https://doi.org/10.1007/s10712-016-9374-2, 2017.

Stammer, D., van de Wal, R. S. W., Nicholls, R. J., Church, J. A., Le Cozannet, G., Lowe, J. A., Horton, B. P., White, K., Behar, D., and Hinkel, J.: Framework for high-end estimates of sea-level rise for stakeholder applications, Earths Future, 7, 923–938, https://doi.org/10.1029/2019EF001163, 2019.

Stephens, A. S., Bell, G. R., and Lawrence, J.: Applying Principles of Uncertainty within Coastal Hazard Assessments to Better Support Coastal Adaptation, Journal of Marine Science and Engineering, 5, 40, https://doi.org/10.3390/jmse5030040, 2017.

Stive, M. J. F.: How Important is Global Warming for Coastal Erosion?, Clim. Change, 64, 27–39, https://doi.org/10.1023/B:CLIM.0000024785.91858.1d, 2004.

Stive, M. J. F., Aarninkhof, S. G. J., Hamm, L., Hanson, H., Larson, M., Wijnberg, K. M., Nicholls, R. J., and Capobianco, M.: Variability of shore and shoreline evolution, Coast. Eng., 47, 211–235, https://doi.org/10.1016/S0378-3839(02)00126-6, 2002.

Thiéblemont, R., Le Cozannet, G., Toimil, A., Meyssignac, B., and Losada, I. J.: Likely and High-End Impacts of Regional Sea-Level Rise on the Shoreline Change of European Sandy Coasts Under a High Greenhouse Gas Emissions Scenario, Water, 11, 2607, https://doi.org/10.3390/w11122607, 2019.

Toimil, A., Losada, I. J., Camus, P., and Díaz-Simal, P.: Managing coastal erosion under climate change at the regional scale, Coast. Eng., 128, 106–122, https://doi.org/10.1016/j.coastaleng.2017.08.004, 2017.

Toimil, A., Camus, P., Losada, I. J., Le Cozannet, G., Nicholls, R. J., Idier, D., and Maspataud, A.: Climate change-driven

coastal erosion modelling in temperate sandy beaches: Methods and uncertainty treatment, Earth-Sci. Rev., 202, 103110, https://doi.org/10.1016/j.earscirev.2020.103110, 2020.

Tucker, W. T. and Ferson, S.: Sensitivity in risk analyses with uncertain numbers, Sandia Report, Albuquerque, New Mexico, Livermore, California, United States, 2006.

University of Hamburg: AR5 Sea Level Rise, available at: https://icdc.cen.uni-hamburg.de/en/ar5-slr.html, last access: 2 May 2021.

van der Pol, T. D. and Hinkel, J.: Uncertainty representations of mean sea-level change: a telephone game?, Clim. Change, 152, 393–411, https://doi.org/10.1007/s10584-018-2359-z, 2019.

Verschuur, J., Le Bars, D., Katsman, C. A., de Vries, S., Ranasinghe, R., Drijfhout, S. S., and Aarninkhof, S. G. J.: Implications of ambiguity in Antarctic ice sheet dynamics for future coastal erosion estimates: a probabilistic assessment, Climatic Change, 162, 859–876, https://doi.org/10.1007/s10584-020-02769-4, 2020.

Vitousek, S., Barnard, P. L., and Limber, P.: Can beaches survive climate change?, J. Geophys. Res.-Earth, 122, 1060–1067, https://doi.org/10.1002/2017JF004308, 2017.

Vos, K., Harley, M. D., Splinter, K. D., Simmons, J. A., and Turner, I. L.: Sub-annual to multi-decadal shoreline variability from publicly available satellite imagery, Coast. Eng., 150, 160–174, https://doi.org/10.1016/j.coastaleng.2019.04.004, 2019a.

Vos, K., Splinter, K. D., Harley, M. D., Simmons, J. A., and Turner, I. L.: CoastSat: A Google Earth Engine-enabled Python toolkit to extract shorelines from publicly available satellite imagery, Environ. Modell. Softw., 122, 104528, https://doi.org/10.1016/j.envsoft.2019.104528, 2019b.

Vousdoukas, M. I., Ranasinghe, R., Mentaschi, L., Plomaritis, T. A., Athanasiou, P., Luijendijk, A., and Feyen, L.: Sandy coastlines under threat of erosion, Nat. Clim. Change, 10, 260–263, https://doi.org/10.1038/s41558-020-0697-0, 2020.

Wong, T. E., Bakker, A. M. R., and Keller, K: Impacts of Antarctic fast dynamics on sea-level projections and coastal flood defense, Climatic Change, 144, 347–364, https://doi.org/10.1007/s10584-017-2039-4, 2017.

Wöppelmann, G. and Marcos, M.: Vertical land motion as a key to understanding sea level change and variability, Rev. Geophys., 54, 64–92, https://doi.org/10.1002/2015RG000502, 2016.